

Load Case Selection Technique for Combined Modal Finite Element Approach of High Aspect Ratio Wing Models^{*}

Norzaima Nordin^{1,2}, Baizura Bohari¹, Thinesh Chandrasegaran², Azizan As'arry² and Mohammad Yazdi Harmin^{2**}

¹*Department of Aeronautical Engineering and Aviation, Faculty of Engineering, Universiti Pertahanan Nasional Malaysia, 57000 Sungai Besi, Kuala Lumpur, Malaysia*

²*Department of Aerospace Engineering, Faculty of Engineering, Universiti Putra Malaysia 43400 Serdang, Selangor, Malaysia*

Email address: norzaima@upnm.edu.my (Norzaima Nordin), baizura@upnm.edu.my (Baizura Bohari), thinesh7894@gmail.com (Thinesh Chandrasegaran), zizan@upm.edu.my (Azizan As'arry) and myazdi@upm.edu.my (Mohammad Yazdi Harmin), *Corresponding author: myazdi@upm.edu.my (Mohammad Yazdi Harmin)

ABSTRACT

High aspect ratio wing is known to exhibit high deflection even though at relatively low aerodynamic loading, hence it is susceptible to geometric nonlinearity. Since an integration between the finite element analysis (FEA) of linear and nonlinear static solutions is a time-consuming process, therefore there is much effort to employ the nonlinear reduced order model (NROM) for computational efficiency. One of the options to enable this is by utilising the combined modal finite element (CMFE) approach. However, to date, there are limited guidelines on the generation of load cases to develop the NROM. Therefore, the present work comprehensively proposed a load case selection method as part of the CMFE procedure. The procedure is initiated with a normal mode selection and continued with loading profile selection technique either using individual or combined modes. The result found that the CMFE approach could predict the deflection with reasonable accuracy compared with FEA with small mean error and low standard deviation. The development of loading profile based on combined modes is exceptionally

** To whom correspondence should be addressed, E-mail: myazdi@upm.edu.my

more accurate with relatively less computational time. Therefore, the proposed methodology can be considered as a way forward in developing NROMs via CMFE approach for future works related to highly flexible wing.

Keywords: Combined modal finite element, High aspect ratio wing, Load case selection technique, Nonlinear reduced order models

I. INTRODUCTION

Greenhouse gas emissions from aircraft is one of the major contributors that causes climate change. Due to this, there is much effort to make the aircraft to become more fuel efficient via venturing an improvement in aerodynamic efficiency, specific fuel consumption and possibility in reduction of aircraft structural weight. A review by Afonso *et al.*, [1] has shown that the wing aspect ratio for the commercial jet designs has gradually increased over the past couple of decades. This was due to the fact that, by increasing an aspect ratio of the wing, a higher lift-to-drag ratio could be acquired as a result of the reduction in induced drag parameters [2]. Despite of this benefit, the deflection of the wing will be getting higher and consequently at a much higher aspect ratio, the wing could significantly deflect even though at relatively low in aerodynamic loading. Therefore, for a wing that is within the category of high aspect ratio (HAR), it can easily be prone to geometry nonlinearity, causing the conventional linear finite element solution becoming undesirable to correctly predict its static and dynamic responses.

A number of research have been conducted considering the inclusion of geometric nonlinearity in their analysis. For instance, Rosly & Harmin [3] performed linear and nonlinear finite element analysis (FEA) for the HAR wing models under gravitational loading with the wing positioned in a horizontal arrangement. Their finding shows that by increasing the wing length, which also portrays an increment in aspect ratio, the nonlinear hardening effect was becoming noticeable. Meanwhile, Nordin *et al.*, [4] investigated the effect of follower force by applying the tip force at the high aspect ratio plate. The finding shows that the follower force effect provides a greater plate deflection when compared to its corresponding non-follower force effect in both computational and experimental works.

In another work by Rosly *et al.*, [5] conducted experimental modal analysis for undeformed and deformed configurations of the HAR wing model, whereby the differences in modal attributes were found. This finding was in line with the numerical investigation by Tang & Dowel [6], Patil & Hodges [7] and Harmin & Cooper [8] which shows that

the chordwise and torsional modes of an undeformed configuration have respectively changed into chordwise-torsion and torsion-chordwise modes as the wing deforms in bending shape. The changes were found even more prominent as the bending deformation was at a greater magnitude, revealing a possibility of mode swapping. Therefore, this may cause the flutter speed of the deformed configuration to be different than its undeformed configuration. In the comparison study conducted by Howcroft *et al.*, [9], a number of nonlinear aeroelastic modelling methods were considered and the comparison was also made against its linear HAR wing model. A large difference was found between the prediction of linear and nonlinear analysis in terms of wing deflection, aerodynamic force as well as the root bending and twist moment. Hence, this further strengthens the necessity to include geometric nonlinearity in order to accurately model the HAR wing system. Nevertheless, since most of the available methods are still computationally demanding to be performed, consideration in the development of reduced order models has become an important aspect for computational efficiency. This was also one of the conclusions drawn from the review by Afonso *et al.*, [1].

Previous studies have successfully shown that the nonlinear reduced order model (NROM) method can reduce the computational time by minimising the problem's scale, thus analysing the characteristics of the geometrical nonlinearity of the wing model [8]–[11]. One of the highlighted approaches that utilise the finite element packages to develop NROM is using the combined modal finite element (CMFE) approach which is based upon the work of McEwan *et al.*, [12]. In the researcher work, the normal modes of the underlying linear system were chosen as a basis vector to consider the reduced basic approach. The first attempt that employed CMFE in the aeroelastic analysis was by Harmin & Cooper [8] utilising the structural ROM and coupled with the aerodynamic model using modified aerodynamic strip theory at HAR wing model. This method was then further extended by Xie *et al.*, [10] and Chao *et al.*, [11] providing a solution to gust response aeroelastic problems based on the improvement of NROM via the CMFE approach. Chao *et al.*, [11] proposed using seven (7) modes to recover the large deflection in the development of NROM. In other work presented by Chandrasegaran *et al.*, [13] three types of loading were demonstrated to simulate two modes (bending and torsional) for NROM production. Similar work was performed by Nordin *et al.*, [14] using the same type of loading compared to NROM with and without follower force effects. These studies show a good accuracy with a minimal mean error comparing the results from NROM via the CMFE approach with the conventional FEA. However, the researcher extended the NROM via CMFE work by considering the effect of follower force and found a greater deflection demonstrated by the follower force than the wing

model without consideration of follower force. It was observed that from a previous study, most researchers had ventured into using nonlinear static data as the load case to predict the nonlinear static deformation. As for now, there is only a vague description of the criteria for the load case force selection from the previous studies. Based on these study gaps, this paper would venture into comprehensive load case selection guidelines to provide future researchers with a more intrinsic guideline to base their load case selection. The study would also come up with the development of NROMs associated with load case based on eigenvectors of the wing models which ideally would benefit the researcher with the option to tailor the load case typing according to their needs.

II. METHODOLOGY

The present work employed the finite element (FE) solutions of MSC NASTRAN and integrated with computer programming for a faster and economic purpose in describing the NROM via the CMFE approach. The objective is to propose several improvements in the normal mode and load case selection technique to enable the CMFE approach to be employed efficiently under the scope of static aeroelastic cases. Four stages are involved, starting with the initial stage to identify the design constraint of this research work. This procedure is essential for the feasibility study of wind tunnel application and also to set constraints for the present study. In the second stage, the static aeroelastic analysis with MSC NASTRAN solution code, SOL 144 was performed to extract the aerostatic load under specified flight conditions. The corresponding load vector will then be utilised as an input load for the linear and nonlinear static analyses using solution code, SOL 101 and SOL 106, respectively. For validation of the extracted load vectors, the deflection results from this linear analysis are to be verified back with the deflections from the static aeroelastic analysis, hence instilling confidence to be employed in the nonlinear static analysis.

The third stage is required for the NROM establishment using the application of the CMFE approach. This procedure consists of two consecutive sub-procedures: (a) normal mode and load case definition and (b) application of CMFE for the nonlinear static aeroelastic condition. For the normal mode and load case definition, the procedure is initiated with the normal mode analysis and followed by the analysis for the mode selection. The selection procedures were proposed to determine the load cases in order to develop NROMs to predict nonlinear static deformation in terms of bending and twist deflections. Once the load cases are determined, the CMFE approach is then employed to describe the NROM equations by utilising the backward regression method from a solution of nonlinear static analysis for a range of prescribed loading cases. Finally, the last stage is required in order to ensure the effectiveness of the developed NROM equation. The resulting bending and twist deflection from the CMFE based NROM equation is validated with nonlinear static deflection results in terms of mean error and standard deviation.

2.1 Design Constraints

The development of the HAR wing simulation model is mainly based on the actual HAR wing experimental model use in the wind tunnel application (future work). The design of the wing model is derived from the following constraints; (a) dimension of the wind tunnel test section: 1 m x 1 m x 3 m (height x width x length), (b) maximum allowable speed and (c) aerodynamic performance of the wing (stall angle). The expected wing deflection has to be within the size of the wind tunnel test section. The wing will be placed as an undeformed configuration (centre part of the test section), this will leave a margin of ± 0.5 m between the wing model and the wind tunnel wall. As a result, the maximum bending deflection of each case must be set to be less than 0.4 m in the simulation work, as well as in the experimental work later. As for the twist rotation, the maximum value of twist rotation must be less than 0.18 radians considering the stall angle of the airfoil used (NACA 0012) should be less than 11° .

2.2 Finite Element Analysis

The wing models with aspect ratios, AR-8, AR-12 and AR-16 are used for the present work. The model consists of three components: the spar, ribs, and fairing, based on the wing model from Rosly & Harmin [3]. Figure 1 shows a general representation of the structural FE and aerodynamic models developed via MSC NASTRAN finite element entry.

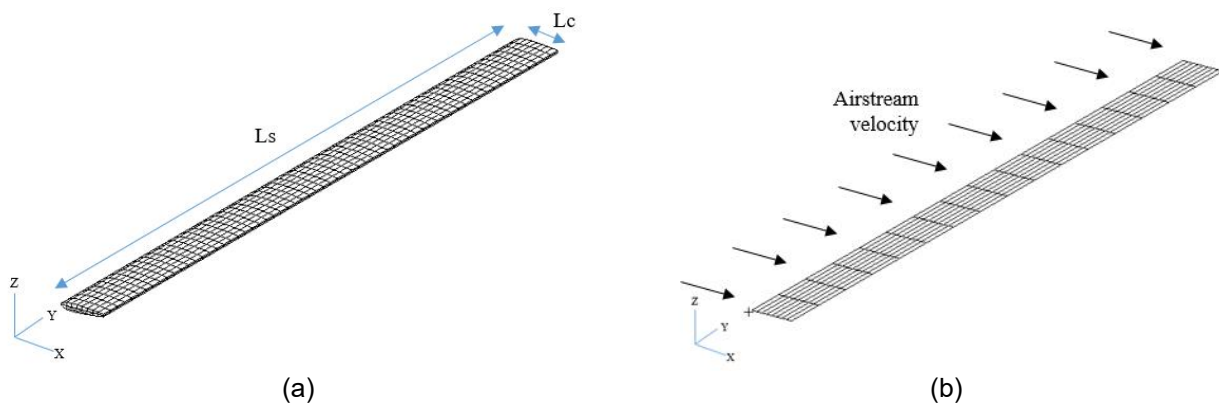


Figure 1 (a) Structural and (b) aerodynamic panel of finite element wing

In FEA material entry, the spring steel material of the spar component is defined as a linear isotropic material. The ABS material of the rib components is defined as shell element anisotropic material and the styrofoam material of the fairing components is defined as a solid element anisotropic material. Since the scope of this paper is only considering for subsonic region, the aerodynamic model of the doublet lattice method (DLM) is employed by MSC NASTRAN on these aerodynamic panel elements. Integration between the structural and aerodynamic model was performed through an interpolation method known as splining (SPLINE1 entry). Therefore, along with the finite element structural model entry, this provides a complete representation of the aeroelastic model.

The static aeroelastic analysis is defined as a flexible structure model that deflects under the applied loads resulted

from aerodynamic forces. This analysis is simulated using solution code, SOL 144 via MSC NASTRAN aeroelastic module. The static aeroelastic analysis aims to extract the aerostatic load under specific flight conditions, which will become an input to run the linear static (SOL 101) and nonlinear static analysis (SOL 106). The linear and nonlinear static analyses are calculated in terms of bending and twist deflection, which will later be compared with the CMFE data.

2.3 NROM via CMFE Approach

NROM is developed using the aforementioned load cases via the CMFE technique and backward regression analysis. The NROM equation undergoes a backward elimination process to optimise the equation without compromising on its accuracy. With the NROM equation characterised by the nonlinear stiffness term, the force input in modal space can be inserted to obtain the corresponding modal displacement value. The modal displacement value then can be translated into physical displacement by utilising the eigenvector of the model used to characterise the equation. The output value is then verified with the FEA data to calculate its accuracy in terms of mean error and standard deviation. The mathematical modelling used by Harmin & Cooper [15] for the static system equation, where $[E_L]$ is assembled linear stiffness matrices of size $NR \times NR$; $\{F\}$ is the $NR \times 1$ applied modal force; $\{E_{NL}(p)\}$ is a polynomial form as the product of N^{th} order modal displacements multiplied by the yet to be defined nonlinear stiffness coefficients and p is the modal displacement.

$$[E_L]\{p\} + \{E_{NL}(p)\} = \{F\} \quad (1)$$

The left-hand side of the equation consists of the restoring stiffness force for both linear stiffness as well as nonlinear stiffness. By rearranging Equation 1:

$$\{F\} - [E_L]\{p\} = \{E_{NL}(p)\} \quad (2)$$

From the equation above, let:

$$[D] = [\{F\} - [E_L]\{p\}] \quad (3)$$

where D is $1 \times NL$ vector; NL is the number of load cases considered for the investigation. Since $\{E_{NL}(p)\}$ is a polynomial function hence the matrix is split into:

$$\{E_{NL}(p)\} = [p^2 \quad p^3] \begin{bmatrix} A_1 \\ A_2 \end{bmatrix} \quad (4)$$

where A_1 and A_2 are the constants in the polynomial equation. For this study, the polynomial order up to the 3rd order is sufficient to characterise the wing model's nonlinear characteristics. However, the polynomial can be tailored fit according to the accuracy of interest of the wing model deformation prediction. Hence, the polynomial constants can be determined by:

$$\begin{bmatrix} A_1 \\ A_2 \end{bmatrix} = [D] [p^2 \quad p^3]^{inv} \quad (5)$$

where $[p^2 \quad p^3]^{inv}$ is the pseudo-inverse of the $[p^2 \quad p^3]$ matrix. Once the coefficients of the polynomial are determined, the NROM equations can then be formed. In order to optimise the equation, a backward elimination procedure is carried

out. Then, the Newton-Raphson method analysis is deployed on the NROM equation to calculate the modal displacement for a defined force. The modal force can be obtained by referring to Equation 6 where the ψ is the $N \times NR$ matrix of the linear mode shapes of the selected mode while the physical displacement, x can be obtained by referring to Equation 7.

$$\{F\} = [\psi] \{F\} \quad (6)$$

$$[x] = [\psi] [p] \quad (7)$$

The accuracy of the NROM is verified with the conventional FEA analysis. The accuracy is evaluated by calculating the mean and standard deviation of the error for each case and is displayed graphically.

2.4 Load Case Selection Technique

The significant contribution of this study is to provide a detailed procedure for generating the load cases in order to develop the NROM equations via the CMFE approach. The procedure is initiated with the normal mode selection technique. Each normal mode is classified into one of three modes categories; bending mode, torsional mode and in-plane mode. The normal mode analysis is conducted using the MSC NASTRAN solver with the solution code, SOL 103. Figure 2 shows examples of the bending and torsional modes considered for the analysis.

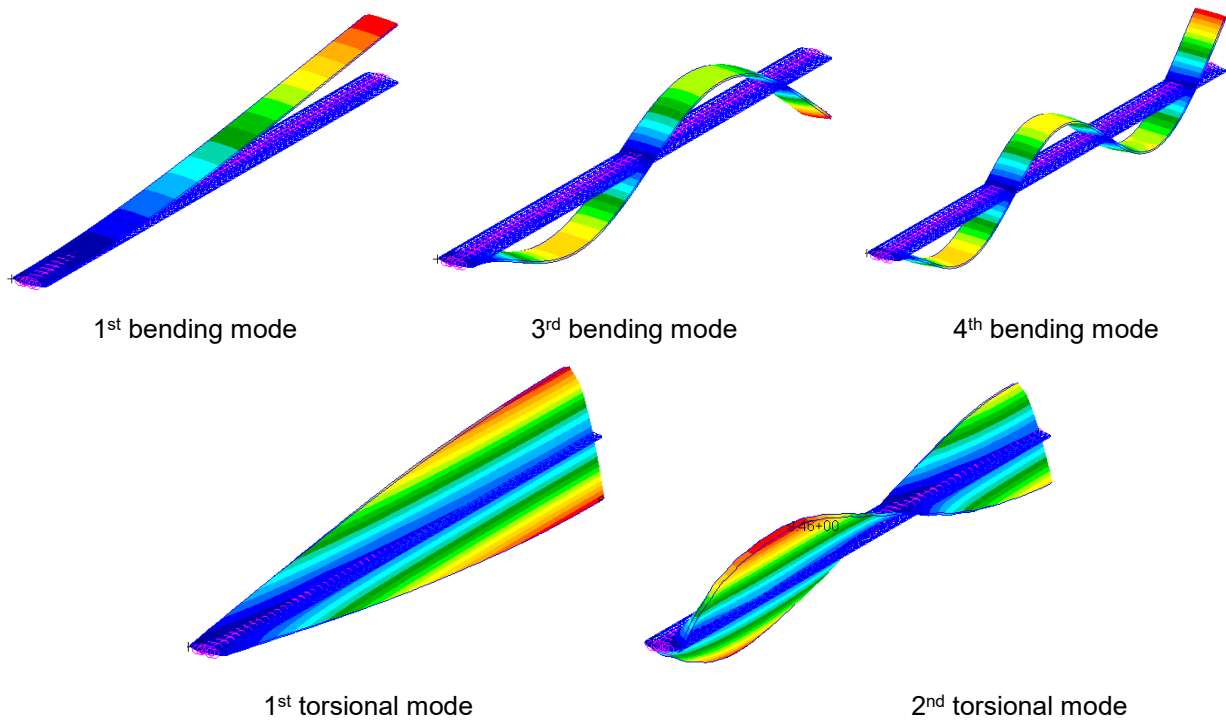


Figure 2 Categories of mode shapes

The modes that contribute significantly to the NROM equation must be identified when developing the CMFE NROM equations in order to obtain the accuracy of NROM equations. Hence, two analyses are conducted to investigate the contribution of each mode selection: (a) investigation by modal displacement and (b) investigation by NROM equation development. After selecting the significant normal modes, the loading profiles were defined. Three types of loading

profiles are considered in this study. The first loading is based on the selected bending mode, the second loading is based on the selected torsional mode and the third loading combines both the selected bending and torsional mode loading profiles. An overview of the load case definition procedure is presented in Figure 3. The highlighted (yellow box) is the new proposed method for CMFE improvement.

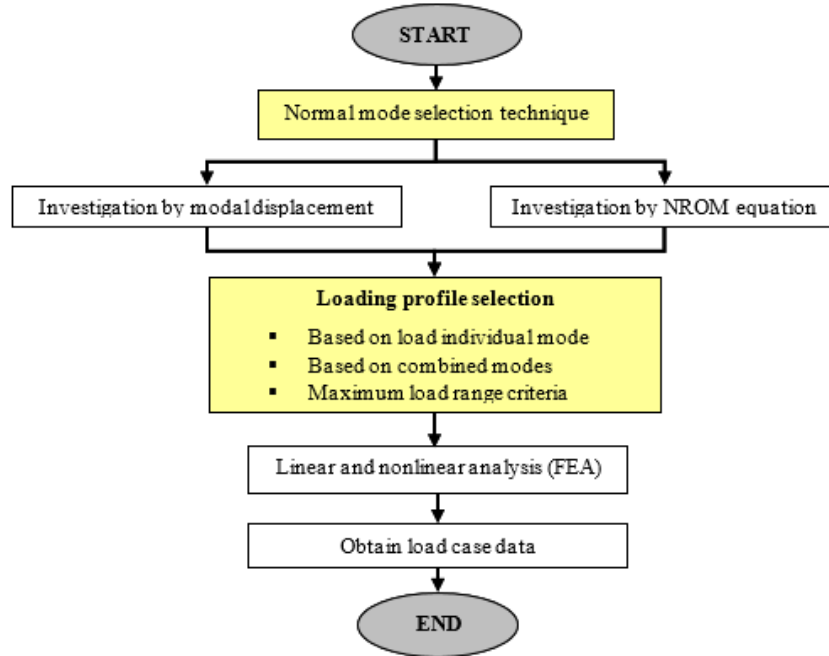


Figure 3 Flowchart of the loading case definition procedure

Loading Profile based on Individual Modes. The first loading profile describes a normalised distributed force that acts on the HAR wing plate to simulate the first bending mode. Meanwhile, the second loading profile describes a normalised distributed force to simulate the first torsional mode. The normalisation procedure is carried as such:

$$F \frac{(\psi)_i}{\max(\psi)_i} = [F] \quad i = 1, 2, 3 \dots \quad (8)$$

where $(\psi)_i$ is the $N \times 1$ eigenvector matrix of the selected mode, $\frac{(\psi)_i}{\max(\psi)_i}$ is the normalised eigenvector, F is the maximum possible force value and $[F]$ is the $N \times 1$ normalised distributed force. The linear and nonlinear static analysis is carried out on the HAR wing model with the loading profile based on individual mode as input. The tip deflection due to the load for the linear and nonlinear static analysis is plotted to ensure the range of force selected covers both the linear and nonlinear region in order to imbue these properties in the NROM equations.

Loading Profile based on Combined Modes. This profile is presented to simulate a combination of bending and torsional effect on the wing models. A force distribution normalised concerning the selected bending and selected torsional mode is described to characterise a bending and twist deflection on the wing model as shown in Equation 9. The tip deflection and tip rotation of the forces are plotted to analyse the nonlinearity of the HAR wing model.

$$F \frac{([\psi]_{i_B} + [\psi]_{i_T})}{\max([\psi]_{i_B} + [\psi]_{i_T})} = [F] \quad (9)$$

where $[\psi]_{i_B}$ is NR x 1 eigenvector matrix of the selected bending mode, $[\psi]_{i_T}$ is NR x 1 eigenvector matrix of the selected torsional mode, $\frac{([\psi]_{i_B} + [\psi]_{i_T})}{\max([\psi]_{i_B} + [\psi]_{i_T})}$ is the normalised eigenvector, F is the maximum possible force value and $[F]$ is the NR x 1 normalised distributed force.

Criteria of Load Case. Apart from loading profile determination, this paper also emphasises the importance of having a guideline for the load case selection to ensure that other researchers can develop the NROMs more conveniently. The load case selected is based on these criteria:

- (a) The load case must cover both the linear and nonlinear deflection of the wing model.
- (b) The load case deflection of the wing model should be at 20% more than the maximum deflection of the nonlinear static wing deflection.
- (c) As for the twist deflection of the wing model, the stall angle of the airfoil can be used as the maximum twist deformation of the wing model.
- (d) From the selected highest load case, a set of range of cases are derived by reducing the magnitude of the highest load case force to the lowest load case force which should characterise the linear region of the deformation.

III. RESULTS AND DISCUSSION

3.1 Static Aeroelastic, Linear Static and Nonlinear Static Analysis

The static aeroelastic analysis is conducted by defining the velocity and angle of attack (AoA), followed by the linear and nonlinear static analyses utilising the static aeroelastic load vector as input. Prior to the nonlinear static analysis, the deformations obtained from the aeroelastic static analysis were cross-verified with the deformations under the linear static analysis at a similar loading. This ensures that the load vectors extracted from the static aeroelastic can be used confidently in the nonlinear static analysis. Figure 4 shows the tip bending and twist deflections for the selected AoA and selected velocity with cross verification plotting of the static aeroelastic and linear static analysis for aspect ratio, AR-16. The degree of nonlinearity of the wing models can be observed in these figures. The corresponding tip deflection was plotted to analyse the wing models nonlinear properties. Nevertheless, the procedure to analyse the static aeroelastic, linear and nonlinear static analysis using the conventional FEA method was very time-consuming. However, the process was still initiated to observe the impact of the nonlinear properties in the wing model to the deformation of the wing model under a certain loading. A similar methodology was also employed to the other aspect ratios; AR-8 and AR-12. Both aspect ratios exhibit nonlinear properties even though the results are less significant than the AR-16 wing model. These figures reinstate the importance of the study in emphasising the nonlinearity of the HAR wing model.

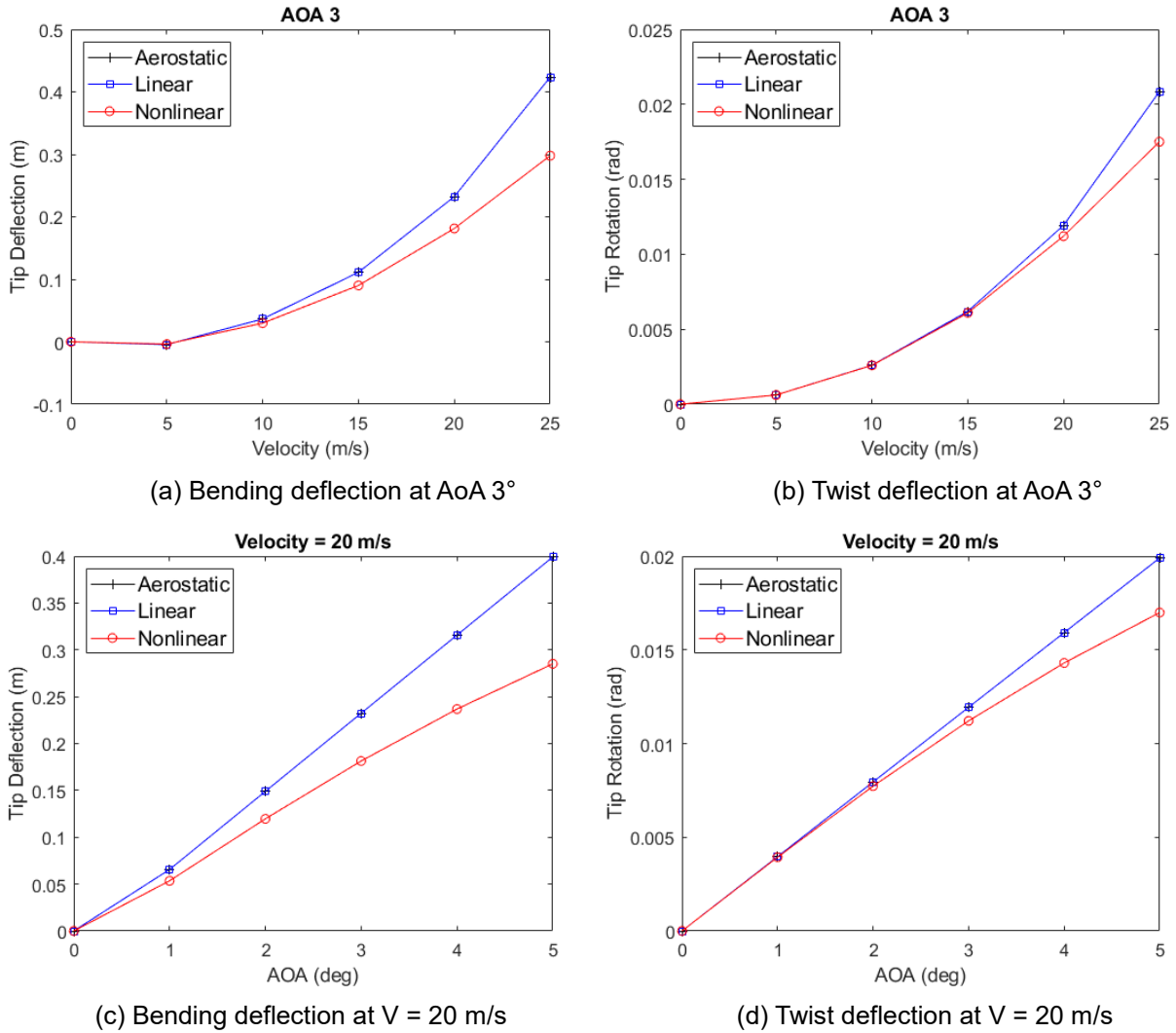


Figure 4 Tip deflection of the static aeroelastic, linear and nonlinear static analyses (AR-16)

3.2 Normal Mode Selection

The selection of normal mode is the utmost important aspect to be considered in order to ensure the accuracy of the NROM equations. The aspect ratio of the AR-16 wing model was selected due to its high degree of geometric nonlinearity. Table 1 shows the results of the modal displacement under the aeroelastic static condition of velocity 20 m/s at AoA 3° for the first eight (8) bending modes and two (2) torsional modes. The first bending mode is much more impactful in the modal displacement characterisation of the deflection compared to the other bending modes and the first torsional mode gives a more impact on the modal displacement compared to the 2nd torsional mode. However, the analyses above give the results assuming that the nonlinear static profile has a similar profile to that of the linear static profile. In order to confirm the effectiveness of the selected modes in predicting the bending and twist deflection of the wing models, another analysis is to be considered in the CMFE procedure. As for the load case selected to develop the NROM equation, the solutions for the nonlinear static analysis at AoA 3° with a velocity range from 5 m/s to 25 m/s is performed.

Table 1 Modal displacement of the AR-16 for the first 8 bending modes and 2 torsional modes

Mode	Modal Displacement	
	Bending	Torsion
1 st	593.65908	22.86712
2 nd	5.32672	7.37897
3 rd	15.10817	-
4 th	14.28381	-
5 th	14.25461	-
6 th	13.74516	-
7 th	13.38678	-
8 th	13.38678	-

In this work, five load cases were considered to develop the NROM equation. Table 2 shows the NROM equations designated for the first, second and third bending modes with the first two torsional modes. Table 3 shows the mean error of the combined equations in predicting the nonlinear profile of the AR-16 wing model for the static aeroelastic condition at AoA 3°. The first bending mode is significantly important to predict the bending deflection of the wing model. Meanwhile, for the twist deflection, the first torsional mode gives significantly higher accuracy in comparison to the second torsional mode. Therefore, the first bending mode and first torsional mode are significant to be used in predicting the nonlinear static deflection of the AR 16 wing model.

Table 2 NROM equation for selected modes

Mode	NROM Equation
First Bending	$f = 88.157 p_1 + 486.66p_1^2$
Third Bending	$f = (2.717 \times 10^4) p_3 + (1.426 \times 10^7)p_3^2$
Fourth Bending	$f = (1.045 \times 10^5) p_4 + (-6.687 \times 10^7)p_4^2$
First Torsional	$f = (2.537 \times 10^5) p_6 + (2.933 \times 10^8)p_6^2$
Second Torsional	$f = (2.571 \times 10^6) p_{12} + (9.022 \times 10^9)p_{12}^2$

Table 3 Mean error of the NROM equations in predicting the nonlinear profile of the AR-16

Mode of NROM Equations	Mean Error	
	Bending Deflection (m)	Twist Deflection (rad)
First Bending	0.00521	0.015
Third Bending	0.154	0.015
Fourth Bending	0.154	0.015
First Torsional	0.154	0.0013
Second Torsional	0.154	0.015

3.3 Loading Profiles

Based on the results from the mode selection technique, two types of loading profiles were defined for the AR-16 wing model: (a) loading profile based on individual mode and (b) loading profile based on combined modes. The individual loading profile was based on the selection of the single significant modes (bending or torsion modes) identified in Table 3. Figure 5 (a) shows the linear and nonlinear tip deflections of the load case for a series of loads in loading profile 1 (1st bending mode shape). It can be seen that the forces selected were within a range that covers both linear and nonlinear regions hence providing great confidence that the NROM equations were able to cover both of these regions starting from 0.001 N to 0.069 N. As previously mentioned, for the criteria of the load case selection technique, the maximum deflection of the wing model is set up to be 60 % of the wingspan length. For the AR-16 wing model, the wingspan is 0.8 m, hence the maximum tip deflection for the nonlinear static deflection is limited up to 0.48 m. Meanwhile, Figure 5 (b) shows the linear and nonlinear tip rotation of the load case for a series of loads starting from 0.08 N to 0.4 N in loading profile 2 (1st torsion mode shape). The maximum twist angle was set to the stall angle of the NACA 0012 airfoil which is AoA 11° or 0.18 radian. The highest aspect ratio of the AR-16 wing model displays nonlinear twist bending properties that need to be considered for NROM production.

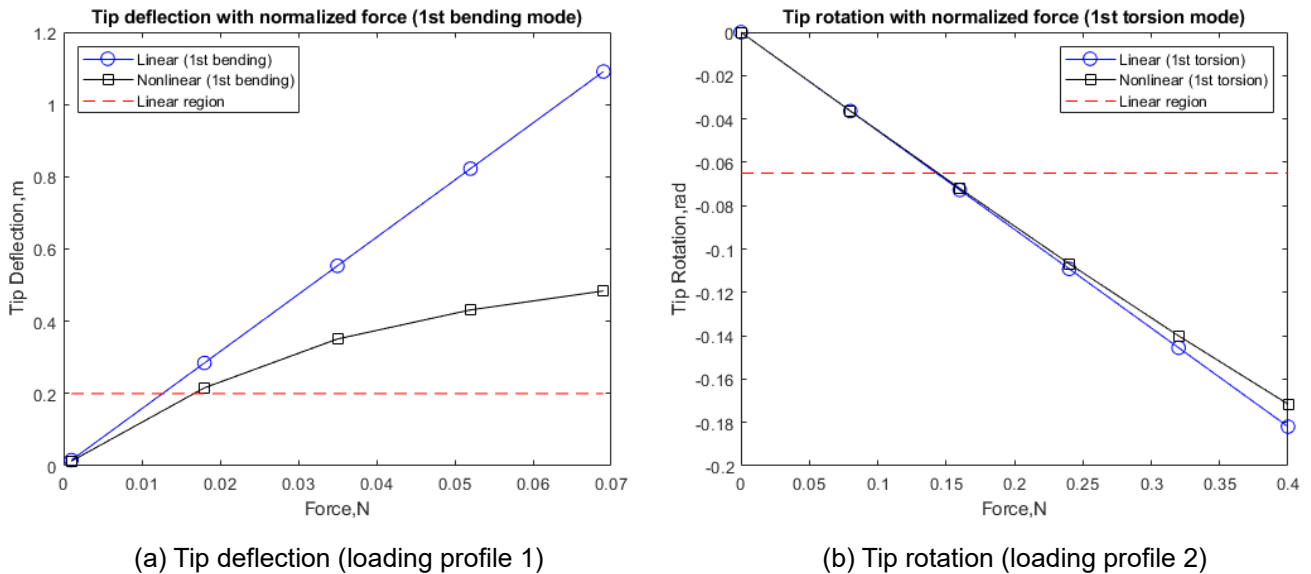


Figure 5 Linear and nonlinear tip deflection and rotation of the AR 16 wing model

Figure 6 shows the linear and nonlinear tip bending and twist deflections of the load case for a series of loads starting from 0.014 N to 0.07 N for a combined mode of loading profiles. The loading profile 3 was developed by multiplying the force to the ratio of the summation of 1st bending and the 1st torsion eigenvectors to the summation of the maximum value of 1st bending and the 1st torsion eigenvectors which is expressed in Equation 9.

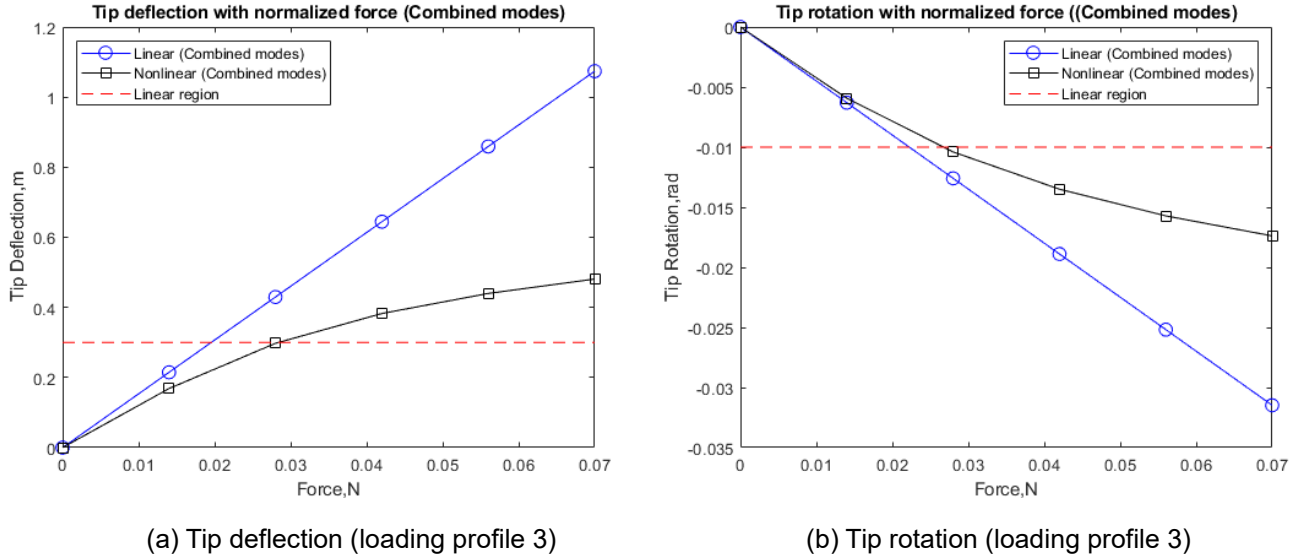


Figure 6 Linear and nonlinear tip deflection and rotation for loading profile 3 of the AR-16 wing model

3.4 Establishment of Complete NROM for HAR Wing Model

The loading profile 1 and loading profile 2 NROMs are categorised as CASE-1, while loading profile-3 NROMs are termed as CASE-2. The nonlinear static aeroelastic deformation, obtained from the FE analysis, is predicted by the NROMs are limited to a tip bending deflection of 50% of the wingspan to limit the nonlinearity of the wing models. The wing model is subjected to velocity up to a maximum of 35 m/s and the AoA varying from 1° to 5°.

Prediction of Static Aeroelastic Nonlinear Static Deformation with NROMs from Loading Profile 1 and Loading Profile 2 (CASE-1). The NROM equation is set till the 3rd order and the NROM equation as shown below:

$$f = 88.157 p_1 + 6725.21p_1^3 \quad (10)$$

$$f = (2.537 \times 10^5)p_6 - (1.38 \times 10^8)p_6^2 \quad (11)$$

where p_1 and p_6 are the modal displacements. These equations are distinguished as the loading profile 1 using the first bending mode and loading profile 2 using the first torsional mode. These NROMs are used to predict the nonlinear static aeroelastic deformation obtained from the FE analysis.

Prediction of Static Aeroelastic Nonlinear Static Deformation with NROMs from Loading Profile 3 (CASE-2). The NROM equation is set till the 3rd order and the NROM equation as shown below:

$$f = 88.157 p_1 + 6695.11p_1^3 \quad (12)$$

$$f = (2.537 \times 10^5)p_6 + (1.799 \times 10^8)p_6^2 \quad (13)$$

where p_1 and p_6 are the modal displacements. These equations are characterised by loading profile 3 using the first bending and first torsional modes. These NROMs are used to predict the nonlinear static aeroelastic deformation obtained from the FE analysis.

Comparison of Static Aeroelastic Nonlinear Static Deformation with NROMs from CASE-1 and CASE-2. Figure 7 and Figure 8 summarise the comparison results of the NROM equations for tip bending and twist deflections in terms of mean error, μ_{err} and standard deviation, σ_{err} for CASE-1 and CASE-2, respectively. In Figure 7, both cases show almost similar trends of graph and value of errors. The only notable highest errors (in meter) occur in the middle to high nonlinear regions for both cases, with a maximum mean error of less than 1 cm. Overall, the disparities are indeed reasonably small compared to the maximum deflection of the wing model. In Figure 8, the developed NROMs are able to predict the twist deflection of the wing model with very high accuracy. The highest mean error was found approximately 0.003 rad for the CASE-1 and the maximum mean error for the CASE-2 prediction is 0.0018 rad. This demonstrates that NROM-CASE 2 is the better option for predicting the twist deformation of the wing model. Meanwhile, Figure 9 shows comparison results between CASE-1 and CASE-2 with conventional FEA nonlinear static data at three ranges of AoA 1°, AoA 3° and AoA 5°. In terms of tip deflection, both approaches have a broadly similar pattern with a CASE-1 and CASE-2 having almost similar tip deflection values. In the prediction of tip rotation, CASE-2 (combined loading profile) shows slightly near the FEA simulation data compared to the prediction of NROM via CMFE using the CASE-1 loading profile.

In overall, these results demonstrate the appropriateness of NROM via CMFE prediction associated with additional improvement via load case selection technique in the nonlinear analysis. Both cases show a good correlation and similar pattern in terms of tip deflections. Nevertheless, in tip rotation analysis, NROM-CASE 2, developed using loading profiles 3 characterised by the first bending mode and the first torsional mode, is exceptionally more accurate than NROM-CASE 1. This analysis highlights that loading profile 3 characterisations of the NROM with the required deformation profile would produce more accurate results than other loading profiles. The selection criteria set can also be seen as a good guideline as the NROMs developed have accurate results, despite the NROM-CASE 2 has more accurate results. The same trend was also observed for aspect ratio, AR-8 and AR-12. Figure 10 shows the comparison results of the NROM equations for tip bending and twist deflections in terms of mean error and standard deviation for CASE-1 and CASE-2 at the highest AoA 5°. Both cases show a similar pattern of the tip deflection and tip rotation accuracy with the value of mean error less than 0.0007 m and 0.008 rad, respectively. The lower aspect ratio wing has high resistivity to twist; hence the nonlinear static profile for the twist deformation is not much different from the linear static profile. For AR-12, it is noted a significant accuracy difference between the two NROMs in the bending deformation. It can be seen that CASE-2 is the better option to predict the bending deformation of the wing model with the least mean error value of 0.006 rad. Similar to the NROMs for the AR-16 wing model, the CASE-2 of the AR-12 wing model which was developed using loading profile 3 characterised by the first bending mode and the first torsional mode, stands out to be significantly more accurate than the CASE-1.

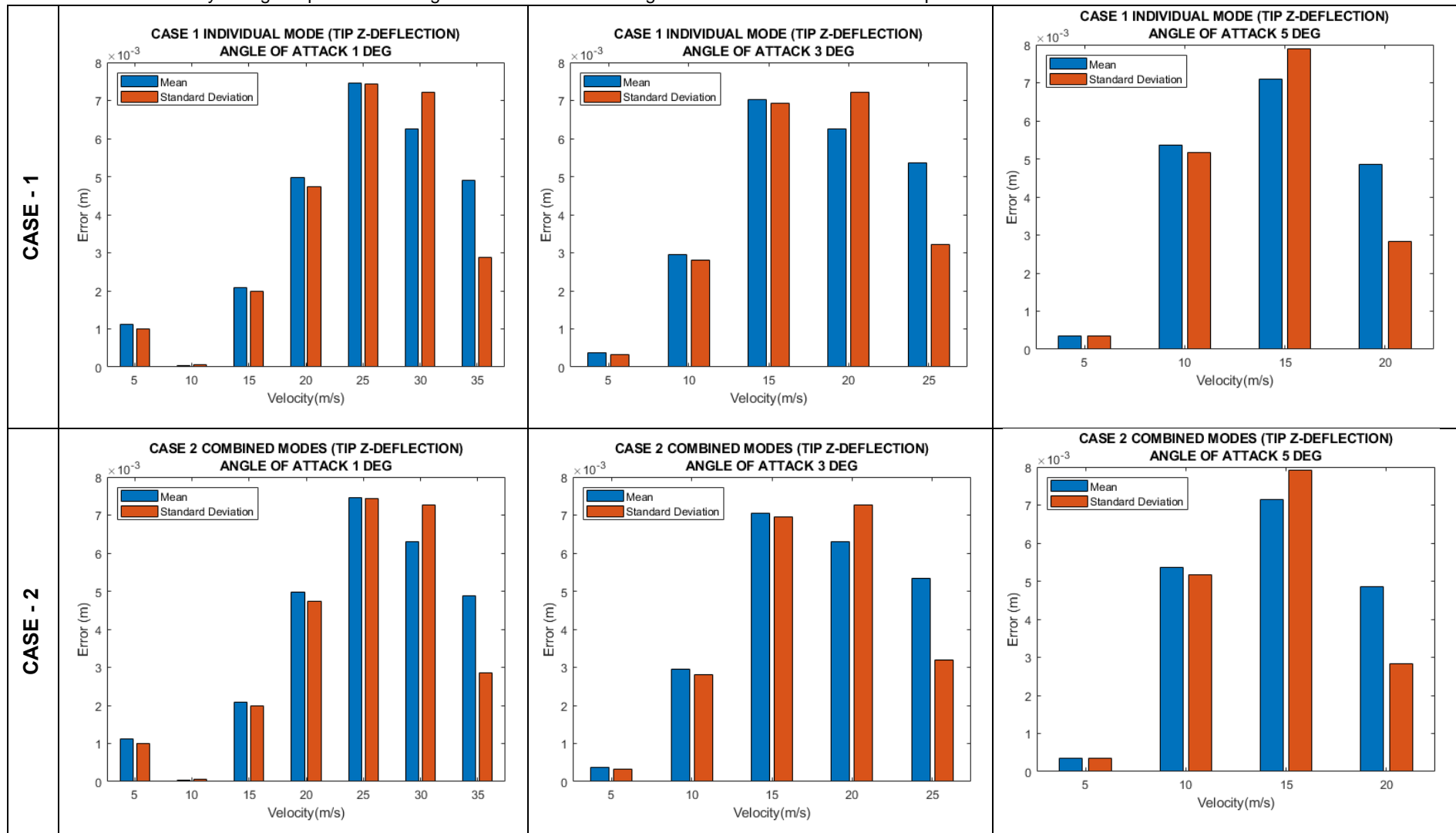


Figure 7 μ_{err} and σ_{err} of NROM prediction between nonlinear static aeroelastic FE and bending deflection for CASE-1 and CASE-2

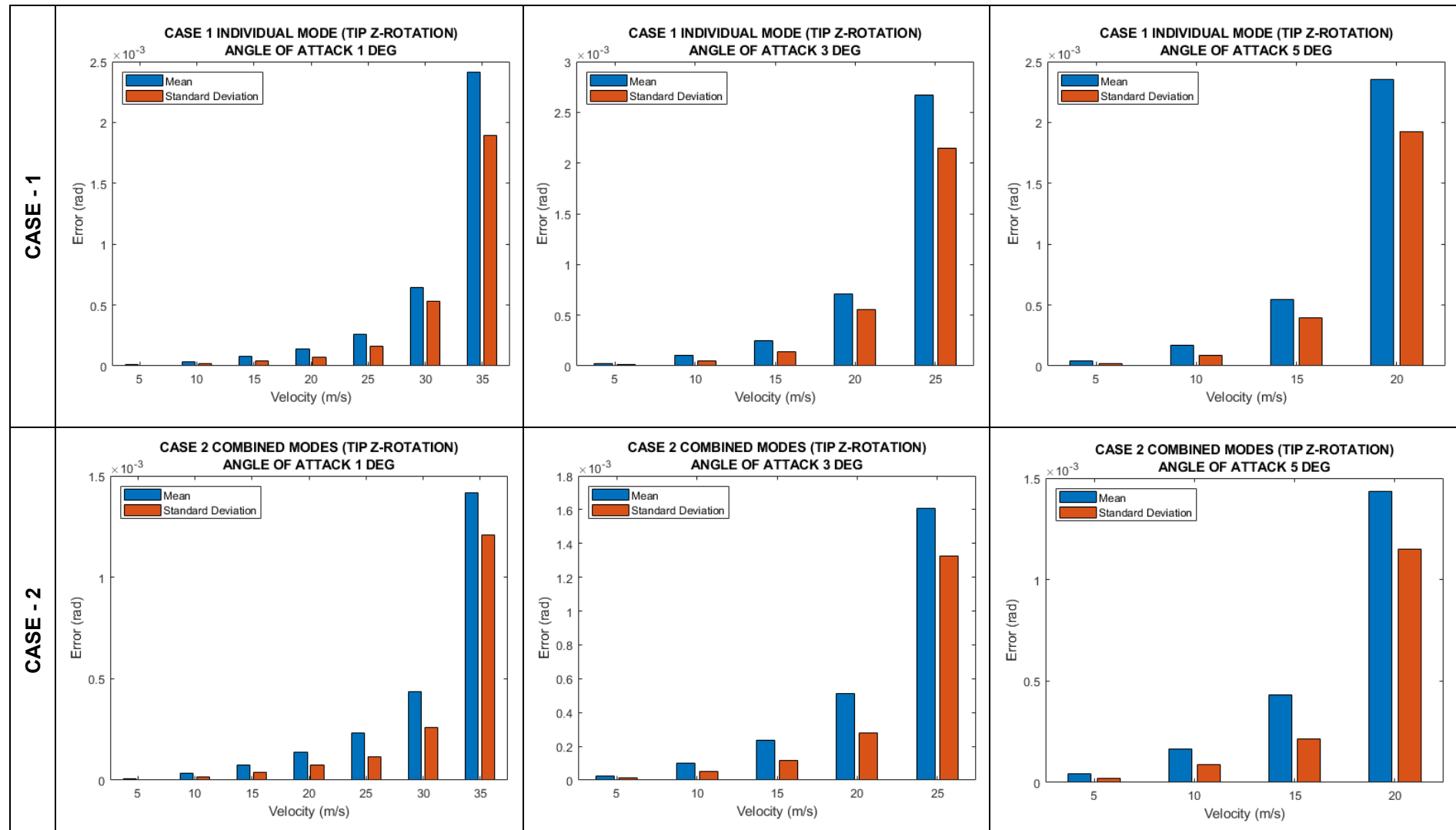


Figure 8 μ_{err} and σ_{err} of NROM prediction between nonlinear static aeroelastic FE to twist deflection for CASE-1 and CASE-2

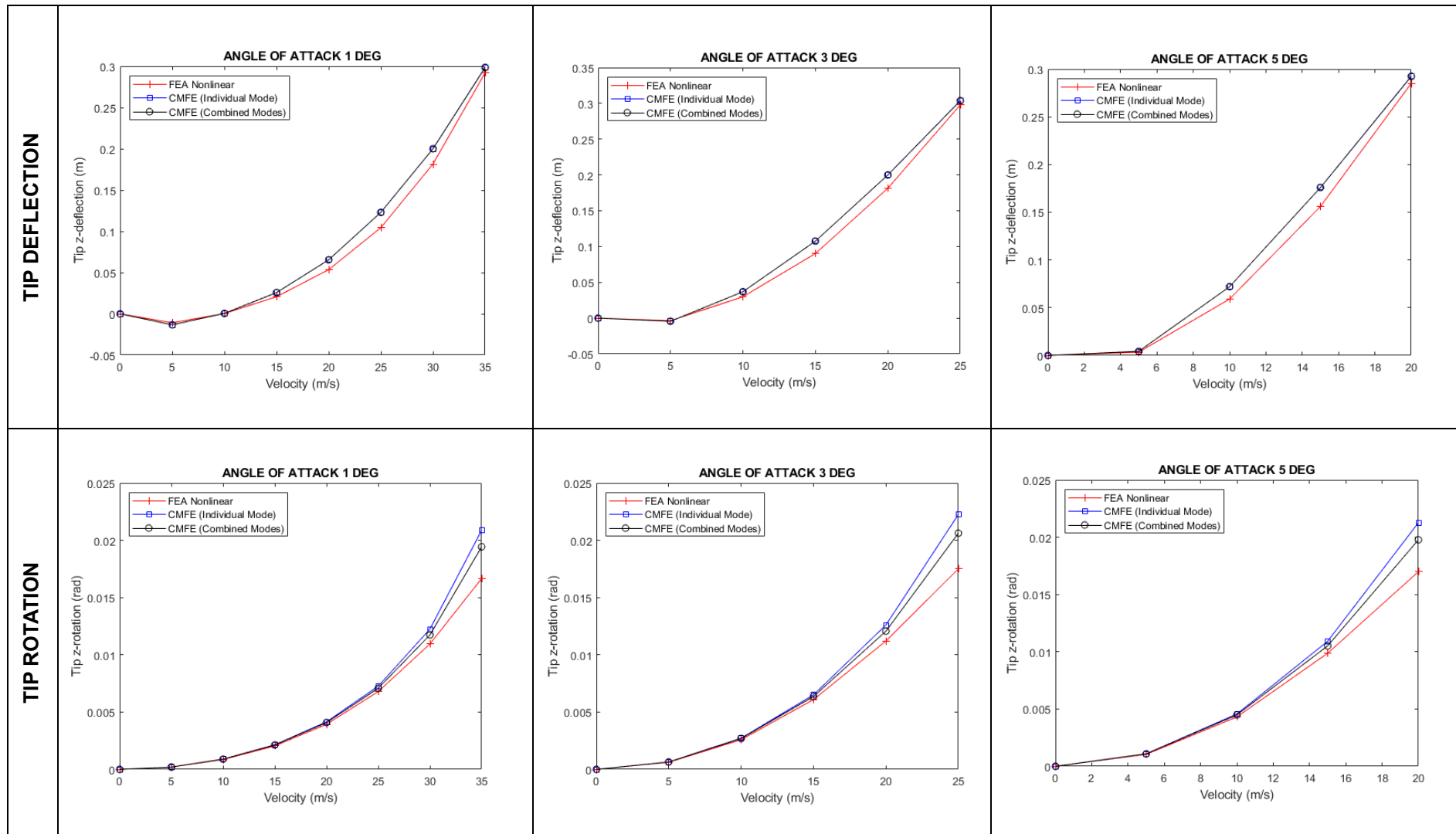
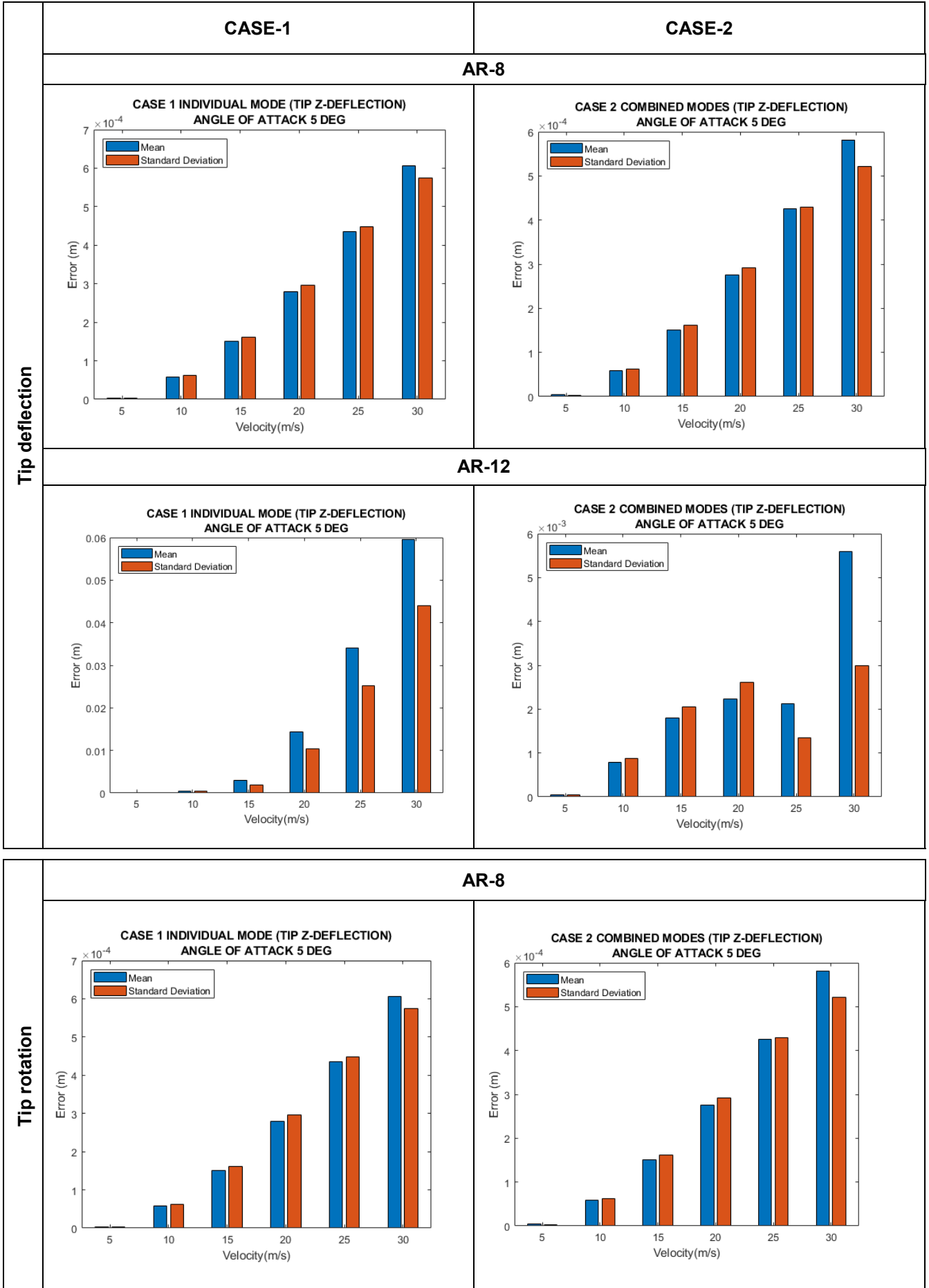


Figure 9 Comparison data of NROM via CMFE prediction for CASE-1 (individual) and CASE-2 (combine) to FEA nonlinear static analysis



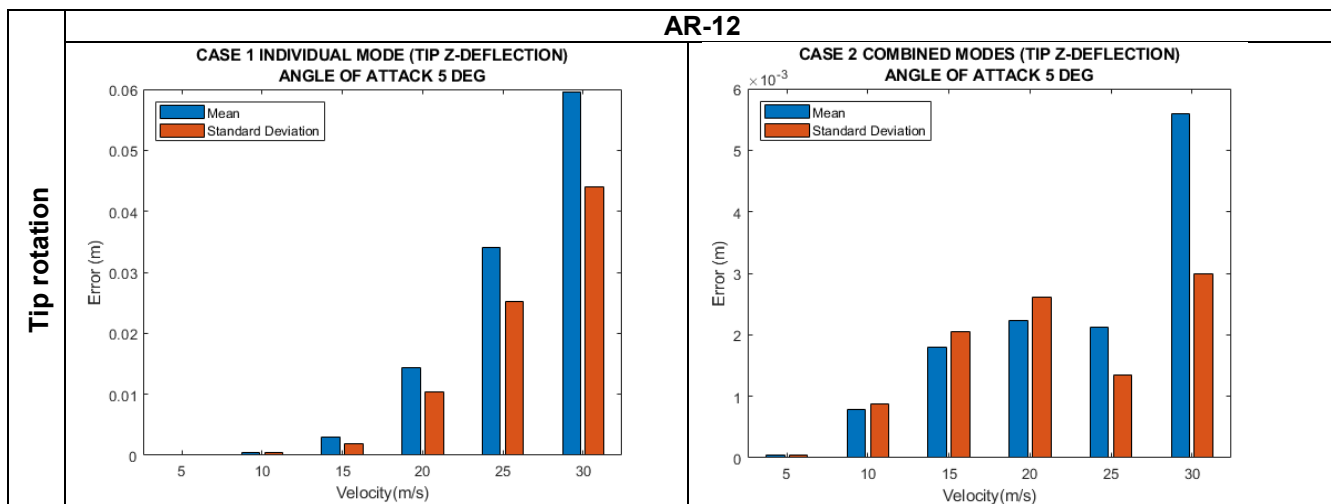


Figure 10 μ_{err} and σ_{err} of NROM prediction between nonlinear static aeroelastic FE for CASE-1 and CASE-2 of AR 8 and AR 12

IV. CONCLUSIONS

This paper aimed to propose comprehensive guidelines on the load cases selection technique and the normal mode selection technique in developing NROM via the CMFE approach. The significant modes selection was based upon modal displacement and NROM equation in nonlinear static analysis at the desired flight load condition. The first bending and the first torsional mode were chosen to characterise the loading profile in the load case selection. Two types of cases with a different selection of loading profiles were chosen: (a) NROM-CASE 1 developed using loading profile based on individual mode and (b) NROM-CASE 2 developed using loading profile based on combined modes. Overall, both cases show a good agreement compared to conventional FEA simulation data in terms of mean and standard deviation error for tip deflections. Nevertheless, the NROM-CASE 2 provides a more accurate result presented by less mean error than the NROM-CASE 1 in terms of tip rotations. Moreover, the development of the loading profile 3 (combination of distributed force using the bending and torsional mode) was much more convenient as the computational time was faster, attributed to only one selection of load cases instead of the individual development which is required to have two different of load cases based on the chosen mode. In conclusion, this work successfully presented the NROM with the CMFE approach as an efficient method to simulate the nonlinearity model and feasible option in the future, thus mitigating the tedious and time-consuming nonlinear analysis using a complex approach.

ACKNOWLEDGMENTS

The authors acknowledge the financial support for the Ministry of Higher Education, Malaysia for supporting this research under grant no. FRGS/1/2020/TK0/UPNM/02/9.

REFERENCES

- [1] F. Afonso, J. Vale, É. Oliveira, F. Lau, and A. Suleman, "A review on non-linear aeroelasticity of high aspect-ratio wings," *Prog. Aerosp. Sci.*, vol. 89, pp. 40–57, 2017.
- [2] J. D. Anderson, "Airfoils, wings and other aerodynamic shapes," in *Introduction to Flight*, 3rd ed., McGraw Hill Education, 2005, pp. 216–221.
- [3] N. A. Rosly and M. Y. Harmin, "Finite element analysis of high aspect ratio wind tunnel wing model: a parametric study," *IOP Conf. Ser. Mater. Sci. Eng.*, vol. 270, no. 1, pp. 1–7, 2017.
- [4] N. Nordin, N. S. M. Rafi, and M. Y. Harmin, "Nonlinear follower force analysis with ground static test validation of high aspect ratio wing," *Lect. Notes Mech. Eng.*, pp. 421–432, 2020.
- [5] N. A. Rosly, M. Y. Harmin, and D. L. A. A. Majid, "Preliminary investigation on experimental modal analysis of high aspect ratio rectangular wing model," *Int. J. Eng. Technol.*, vol. 7, no. 4, pp. 151–154, 2018.
- [6] D. Tang and E. H. Dowell, "Experimental and theoretical study on aeroelastic response of high-aspect-ratio wings," *AIAA J.*, vol. 39, no. 8, pp. 1430–1441, 2001.
- [7] M. J. Patil and D. H. Hodges, "On the importance of aerodynamic and structural geometrical nonlinearities in aeroelastic behavior of high-aspect-ratio wings," *J. Fluids Struct.*, vol. 19, no. 7, pp. 905–915, 2004.
- [8] Y. Harmin and J. Cooper, "Efficient prediction of aeroelastic response including geometric nonlinearities," *51st AIAA/ASME/ASCE/AHS/ASC Struct. Struct. Dyn. Mater. Conf.*, pp. 1–13, 2010.
- [9] C. Howcroft *et al.*, "Aeroelastic modelling of highly flexible wings," *15th Dyn. Spec. Conf. Am. Inst. Aeronaut. Astronaut.*, pp. 1–26, 2016.
- [10] C. Xie, C. An, Y. Liu, and C. Yang, "Static aeroelastic analysis including geometric nonlinearities based on reduced order model," *Chinese J. Aeronaut.*, vol. 30, no. 2, pp. 638–650, 2017.
- [11] A. Chao, X. Changchuan, M. Yang, and Y. Chao, "Efficient aeroelastic response analysis including geometric nonlinearities based on structural ROM," *Int. Forum Aeroelasticity Struct. Dyn.*, pp. 1–15, 2017.
- [12] M. I. McEwan, J. R. Wright, J. E. Cooper, and A. Y. T. Leung, "A combined modal/finite element analysis technique for the dynamic response of a non-linear beam to harmonic excitation," *J. Sound Vib.*, vol. 243, no. 4, pp. 601–624, 2001.
- [13] T. Chandrasegaran, M. Y. Harmin, and N. A. B. Rosly, "Nonlinear reduced order model for aeroelastic static deformations of cantilevered rectangular high aspect ratio wing model," *Int. J. Eng. Adv. Technol.*, vol. 9, no. 1, pp. 924–930, 2019.
- [14] N. Nordin, T. Chandrasegaran, and M. Y. Harmin, "Nonlinear reduced order model of rectangular high aspect ratio wing with and without follower force effects," *J. Adv. Res. Fluid Mech. Therm. Sci.*, vol. 63, no. 1, pp. 117–134, 2019.
- [15] M. Y. Harmin and J. E. Cooper, "Aeroelastic behaviour of a wing including geometric nonlinearities," *Aeronaut. J.*, vol. 115, no. 1174, pp. 767–777, 2011.